EFFECT OF DIVERTOR CONFIGURATION ON PLASMA PERFORMANCE IN JET

The JET Team[1]
(presented by G. Vlases)

JET Joint Undertaking,
Abingdon, Oxfordshire,
United Kingdom.

Abstract

JET has been operating with a new divertor, Mk IIA, since April 1996. Mk IIA is geometrically more closed than Mk I and has better power handling capacity. Pumping performance is improved, and access to high recycling and detached regimes is facilitated. Quasi-steady ELMy H-modes with $H_{89} \sim 2.0$ are produced with moderate gas puffing. The Type I ELM frequency depends primarily on triangularity and the gas puff rate at fixed power, and not strongly on target orientation or divertor magnetic flux expansion. The stored energy loss per ELM decreases with increasing frequency, but can only be reduced below 4% by strong gas puffing, with loss of confinement quality. Highly radiating, detached divertor plasmas can be produced by impurity seeding, but at the expense of confinement degradation and increased Z_{eff} (similar to Mk I results).

1. INTRODUCTION

The JET divertor programme is designed to investigate the effect of divertor geometry on plasma performance in a series of progressively more closed configurations. The programme began with Mark I (1994 - 1995, Fig.1a), presently uses a somewhat more closed divertor (Mark IIA, 1996-1997, Fig.1b), and will conclude with an ITER-specific "Gas Box" configuration (Mark II GB, 1997-1998). In addition to examining the effects of the geometrical positioning of various divertor components, the programme explores the effect of target orientation, X-point height, and flux expansion. Each of the divertors uses a cryopump with a nominal pumping speed of 240 m^3s^{-1}.

The term "closure" in this context refers to the degree to which neutrals recyling from the target plates escape from the divertor region. Closure depends on the divertor plasma temperature, density, and equilibrium geometry as well as on the geometry of the divertor components. In general, a "geometrically closed" divertor will have a larger effect on closure in the low recycling and detached plasma limits, where the ionisation mean free path becomes larger, than in the intermediate high recycling regime. The reasons for increasing closure are (a) to provide easier access to the regime of high volumetric losses in the divertor, thus reducing the target heat loading, (b) to reduce the neutral density in the main chamber, which improves main plasma confinement quality and reduces sputtering of impurities, and (c) to increase neutral pressure in the divertor chamber, thus facilitating pumping. At the same time, improved closure generally leads to reduced flow in the scrape-off-layer (SOL), which results in poorer flushing out of impurities and ash from the main chamber; this can be partly offset by increased pumping. The problem of choosing the correct geometrical closure for a divertor which must operate with Type I ELMs is particularly

[1] See Appendix to IAEA-CN-64/O1-4, The JET Team (presented by J Jacquinot).

difficult because of the great disparity in effective SOL width between and during ELMs. Finally, closure does not prevent the escape of ionized impurities from the divertor region, as they are driven up the field lines by the parallel ion temperature gradient, and are only retained in regions of high SOL flow. Thus, improved closure, per se, will not generally improve impurity retention for seeded divertors.

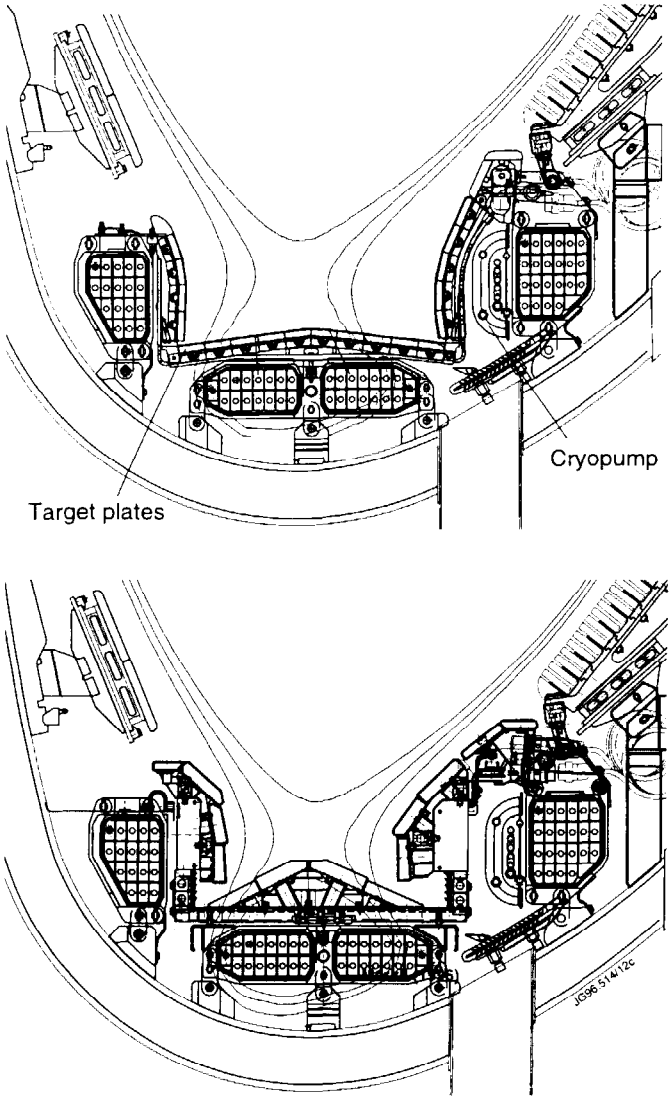

Fig.1 Poloidal cross sectional view of Mark I (top) and Mark II A (bottom).

Much attention was given in the JET Mk I campaign to the study of highly detached, highly radiating seeded divertor plasmas, where it was found possible to reduce the heat flow to the targets to very low levels. However, the confinement quality (H_{89}) was low and Z_{eff} was relatively high at high radiated power fractions with fully detached divertor plasmas [1]. Similar results have been found in other tokamaks [2-4]. Thus the use of this operating scenario for ITER is perceived to be difficult. On the other hand, it has been suggested that time-averaged power loading in ITER operating with divertor plasmas detached only near the separatrix strike points (semi-detached) and Type I ELMy H-modes, which

improves confinement and Z_{eff}, may prove to be satisfactory [5]. In this scenario, the interaction of the Type I ELMs with the target becomes the main concern for the divertor design. In the Mk IIA campaign the study of seeded, radiating divertors has continued, but heavy emphasis has also been placed on the investigation of Type I ELMy H-mode discharges, and the effect of divertor configuration on them.

2. GLOBAL COMPARISON OF MK I AND MK II A

In this section the relative performance of Mk I and Mk IIA is discussed with respect to the principal divertor performance criteria: power handling capacity, approach to detachment, pumping effectiveness, and control of impurities. Mk IIA has a much larger wetted area than Mk I due to the use of large tiles and inclined target plates, and was predicted to have power handling capacity in the non-swept mode 2 - 5 times greater than that of (unswept) Mk I, depending on equilibria used. Infrared measurements of tile temperature show that Mk IIA has exceeded its design goals, and that the overheating of the tiles is not encountered in any normal JET operating scenario.

Increasing divertor geometrical closure should result in access to the high recycling-detachment regime at lower main plasma densities for a fixed power input. Figure 2 shows Langmuir probe measurements of the degree of detachment, defined as midplane SOL electron pressure divided by twice the measured divertor electron pressure [6], for equivalent L-mode density ramp discharges in the two divertors. It is seen that detachment begins at a lower density in Mk IIA than in Mk I, as expected. The "Super Fat" Mk IIA configuration has reduced divertor flux expansion and thus greater leakage than the "Standard Fat", while the HFE of Mk I is even more open. Each of these pulses ended in a density limit disruption, and the density attained decreased as the degree of closure increased. It appears that in general, the "detachment window" between onset of

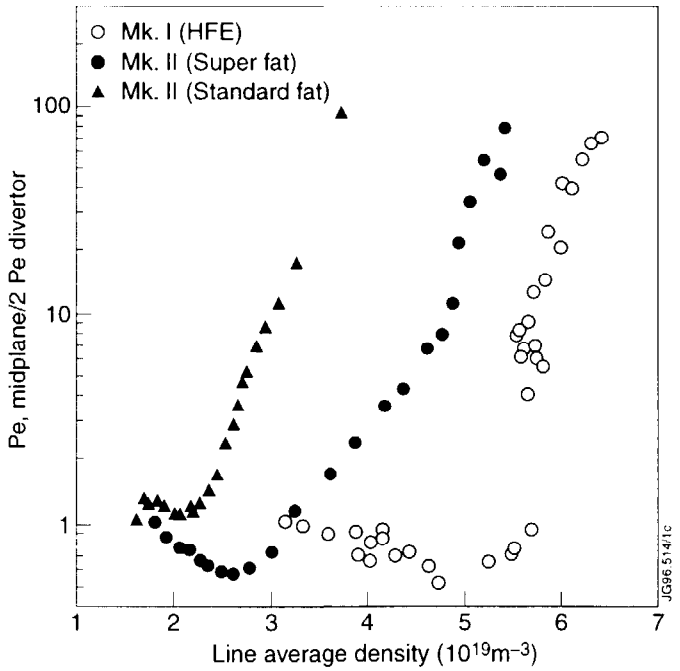

Fig.2 Degree of detachment vs. line averaged density for 3 MW L-mode discharges in Mk I and Mk IIA, showing the effect of increasing closure on the onset of detachment and the density limit.

I_{sat} rollover and disruption is smaller in Mk IIA than in Mk I for ohmic and low power L-mode pulses. (The density limit in H-mode operation is not disruptive and lies near the Greenwald limit in both divertors [7]).

The rate of pumping in Mk IIA is generally higher than in Mk I for equivalent Ohmic [8], L-mode, and ELM-free H-mode discharges, and is less sensitive to strike point position. EDGE2D/NIMBUS simulations indicate that Mk IIA is functioning as a moderate slot divertor and trapping the neutrals near the pumping ports in the lower corners.

Figure 3 shows measured Z_{eff} for Mk I and Mk IIA ELMy H-mode pulses as a function of volume averaged density, and indicates that they are quite comparable. The same statement can be made about the radiated power fraction and main plasma carbon densities. Carbon is the predominant impurity, with beryllium the next largest contributor. Improved closure in Mk IIA should lead to reduced intrinsic impurity content, if most of the sputtering is caused by neutrals originating at the target plates, rather than by direct interaction of plasma with the main chamber walls. The lack of improvement is believed to be due, at least in part, to bypass leakage of neutrals out of the divertor region, which has been increased by the higher divertor neutral pressure. The bypass leaks will be reduced by about 80% during a shutdown in October 1996.

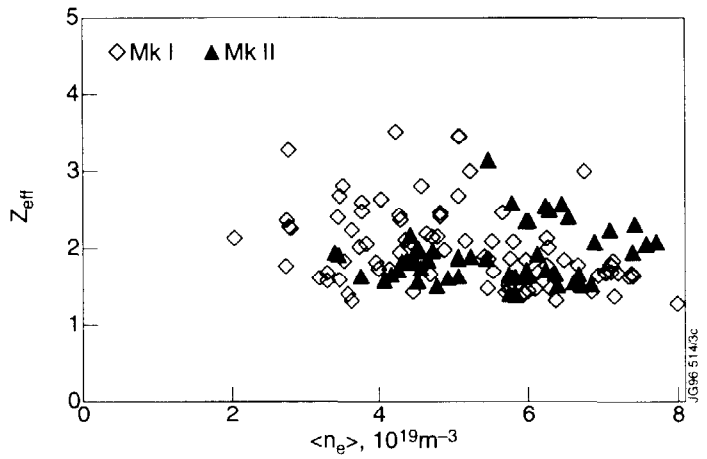

Fig.3 Measured values of Z_{eff} in Mk I and Mk IIA vs <n_e> for Type I ELMy H-mode pulses with total power input ≥ 12 MW.

3. CONFIGURATIONAL EFFECTS ON STEADY STATE ELMY H-MODE DISCHARGES IN MK IIA

3.1 Discharges with beam fuelling only

In order to isolate the effects arising from configurational changes, a series of discharges was carried out with fixed plasma current, magnetic field, and neutral beam power (2.5 MA, 2.5 T, and 12 MW, respectively), in which the target orientation, flux expansion (horizontal target only), and main plasma triangularity were varied. Equilibrium reconstructions (EFIT) of the poloidal flux surfaces in the divertor region are illustrated in Fig.4 for the low triangularity cases. The high triangularity equilibria are nearly identical in the divertor, but differ in the main plasma. It was found that these discharges reached nearly steady state conditions within about 3 seconds of applying the beam power, and that this state was characterized by regularly spaced Type I ELMs. The ELM frequency depends most strongly on triangularity, without reproducible

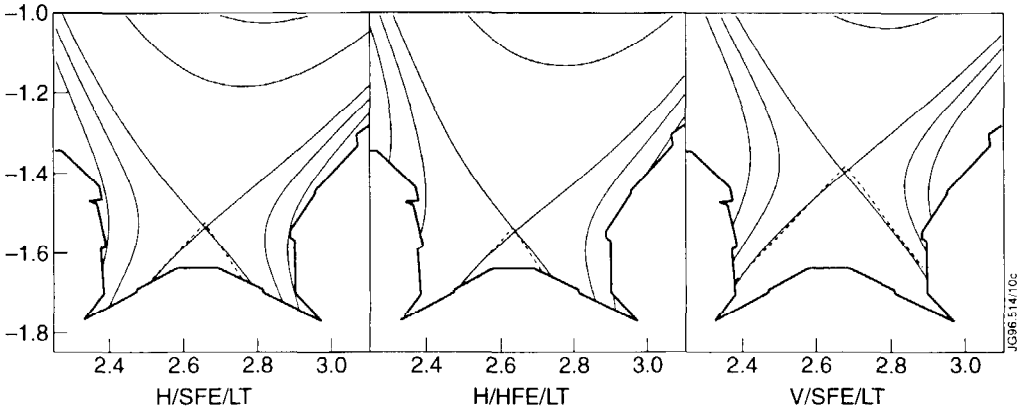

Fig.4 EFIT reconstructions of horizontal standard flux expansion, horizontal high flux expansion, and vertical standard flux expansion equilibria used in the configuration experiments. Flux surfaces shown are 1 and 2 cm distant from the separatrix at the outer midplane.

dependencies on target orientation or flux expansion, as shown in Fig.5. Although the ELM frequency f_E varies by a factor of about 6 for these pulses, the confinement quality, as measured by H_{89}, was independent of both f_E and configuration, as shown in Fig.6. However, the "natural density" at which these beam-fuelled discharges run decreases with increasing f_E. Z_{eff} also drops as f_E

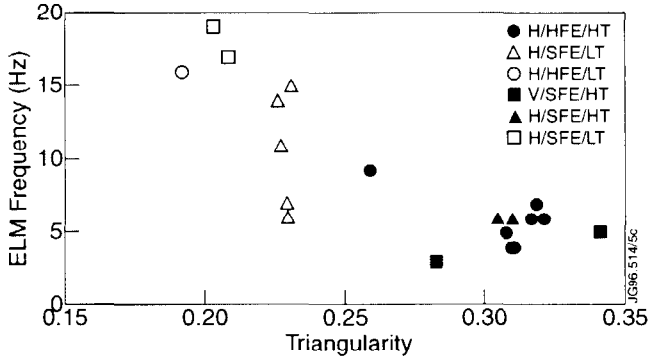

Fig.5 ELM frequency vs. triangularity for pulses with beam fuelling only. The designation of the equilibria A/BBB/CC indicates target orientation, flux expansion (high or standard), and triangularity (high or low), respectively. All of the pulses were run at 2.5 MA, 2.5 T, and 12 MW NB power.

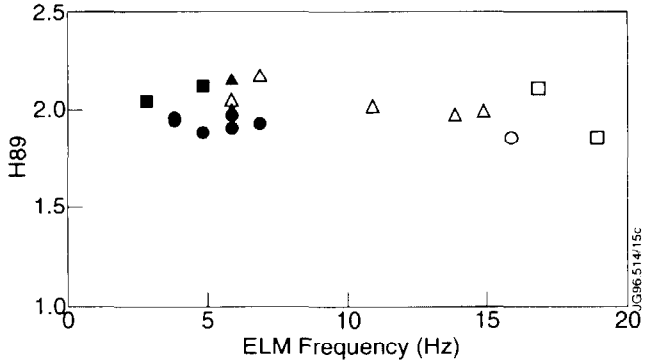

Fig.6 Variation of confinement quality, H_{89}, with ELM frequency, beam-fuelled pulses. The ITERH93-P ELM-free confinement scaling factor, H_{93}, is approximately $0.46xH_{89}$ for the pulses described in this paper.

increases, illustrating the importance of ELMs in purging the edge plasma of impurities. The radiated power fraction in these discharges was quite low for the high ELM frequency configurations, around 25%, increasing at lower ELM frequencies to about 40%.

A set of simulations has been carried out to model the quiescent periods between ELMs of the standard flux expansion horizontal and vertical 12 MW ELMy H-mode pulses described above, using the EDGE2D/NIMBUS code system and a variety of models for the perpendicular SOL transport. It was found that a pinch term gave satisfactory agreement with measured divertor profiles, whereas the customary constant diffusion coefficient model did not. The values used were $\chi_E = 0.2\ m^2s^{-1}$, $D = 0.1\ m^2s^{-1}$, and $V_{pinch} = 4.5\ ms^{-1}$. The present version of the code models the neutral particle behaviour, including the effects of the bypass leaks, more accurately than earlier versions. With this transport model and the bypass leaks included, differences between results for the horizontal and vertical targets are greatly reduced. The target ion saturation current profiles are nearly identical, while the electron temperature profile on the vertical target is flatter than on the horizontal, but not inverted, as shown in Fig.7. The midplane profiles are essentially identical for horizontal and vertical targets, and are quite narrow, with $\lambda_n = 9$ mm, $\lambda_{Te} = 7$ mm, and $\lambda_{Ti} = 12$ mm. These code results are in qualitative agreement with Langmuir probe measurements.

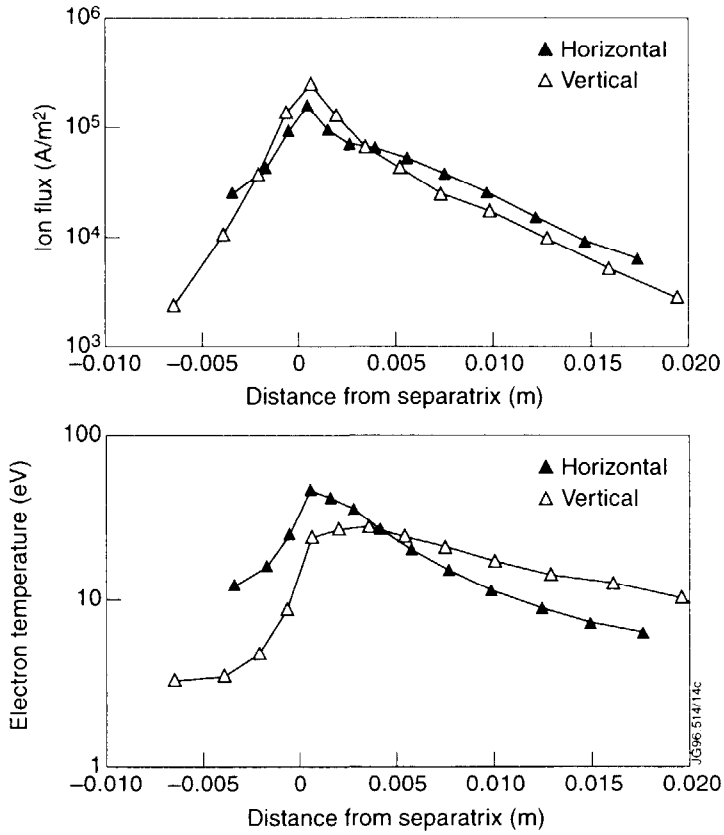

Fig.7 EDGE2D/NIMBUS simulations of target profiles of ion flux (above) and electron temperature (below) for horizontal and vertical pulses corresponding to the experiments. The distance from the separatrix has been mapped to the midplane.

3.2 Discharges with beam fuelling plus D_2 gas puffing

The above series of discharges was systematically repeated with D_2 puffing, which was varied in strength and location. It was found that the ELM frequency was increased by adding heavy fuelling (> 2 x 10^{22} s^{-1}). As puffing is added, the radiated power fraction initially stays the same or decreases slightly. As puffing increases further, the radiated power fraction also increases to a maximum of about 50%, with most of the increased radiation appearing in the divertor/X-point region. The mid-plane neutral pressure rises and the confinement quality declines, with these two variables being clearly correlated, as shown in Fig.8. In this figure the high triangularity standard flux expansion horizontal and vertical configurations appear to be the best, but there may be too few points to be statistically significant. However, as for the beam fuelled cases, the high triangularity discharges have lower ELM frequencies and higher Z_{eff} (Fig.9). The response of the main plasma density to the puffing is described in reference [7].

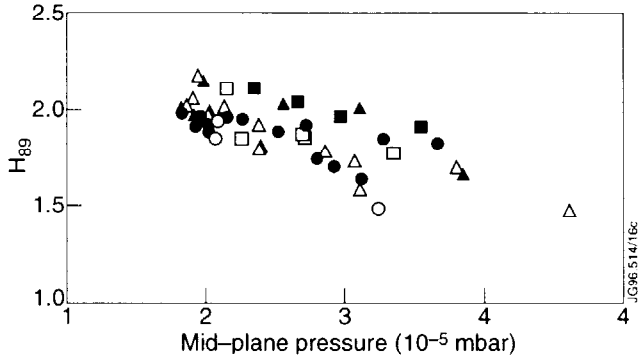

Fig.8 Variation of confinement quality, H_{89} with mid-plane neutral pressure for beam fuelled and D_2-puffed discharges.

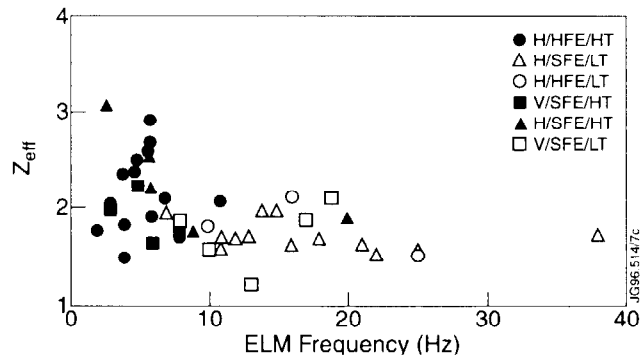

Fig.9 Variation of Z_{eff} with ELM frequency for beam fuelled and puffed discharges.

3.3 Discharges with beam fuelling plus D_2 and N_2 puffing

In order to increase the radiated power fraction beyond the 0.5 available with D_2 puffing, a series of discharges with N_2 seeding was carried out, again in a variety configurations. These discharges attained total radiated power fractions up to about 0.75, and were broadly similar to those carried out with Mk I [1]. As the N_2 puff rate is increased, the character of the ELMs changes and the confinement decreases steadily and makes a gradual transition back to enhanced L-mode levels of H_{89} ~ 1.4, as shown in Fig.10. For these discharges, it appears that the decline of H_{89} with f_{rad} is less severe for the horizontal targets than for the vertical. It was shown by Matthews et. al. [9] that the Z_{eff} values for highly radiating divertor

operation from several tokamaks can be described by a scaling law which can be written approximately as:

$$P_{rad} \sim (Z_{eff} - 1)\langle n_e \rangle^2 S,$$

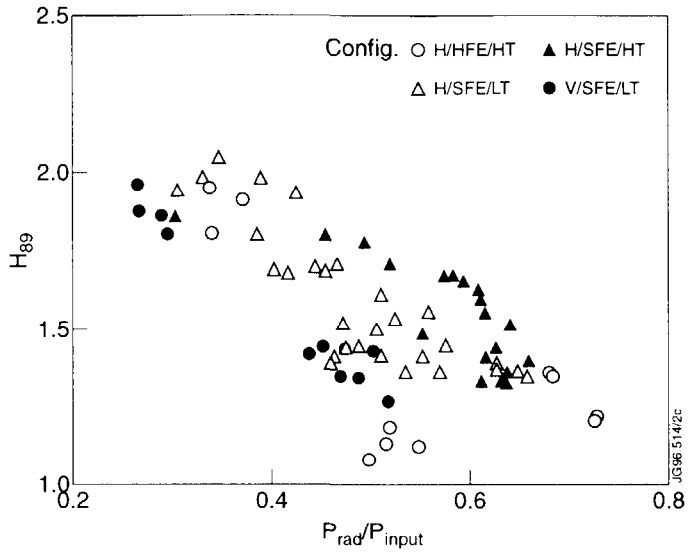

Fig.10 Confinement quality H_{89} vs. radiated power fraction in Mk IIA, for four configurations, with D_2 puffing only ($f_{rad} \leq 0.45$) and D_2 + N_2 puffing.

This scaling is not consistent with the scaling which would be observed if the bulk of the impurities were retained in the divertor. The Mk IIA data for highly radiating pulses fits the same scaling as was found for Mk I, as shown in Fig.11, indicating no improvement of seeded impurity retention, probably for the reason stated in Section 1 of this paper. Neon seeded discharges behave similarly with respect to Z_{eff} scaling, although they display a tendency to radiate more in the main plasma edge than in the X-point region, which reflects the tendency of neon to radiate less than N_2 at low T_e.

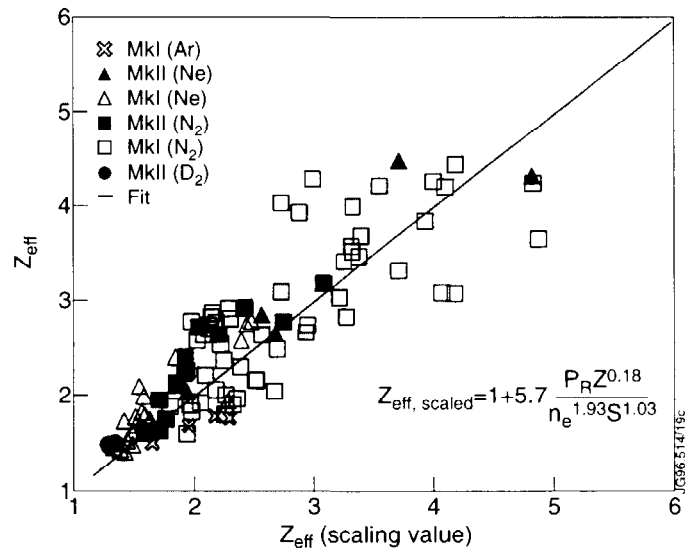

Fig.11 Measured Z_{eff} vs. $Z_{eff,scaled}$ for JET radiative discharges in Mk I and Mk IIA for a variety of seed gases.

4. DETAILED STUDIES OF TYPE I ELMS

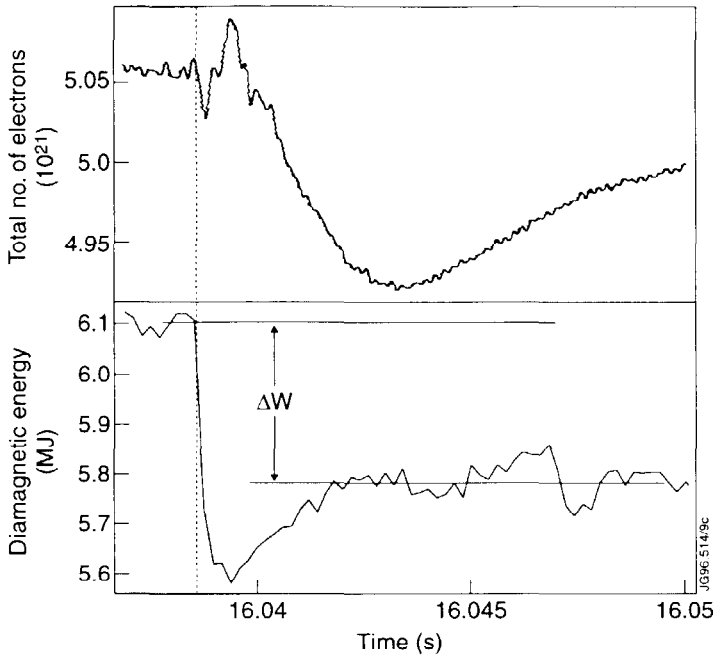

Fig.12 Traces of total particle inventory and stored energy vs. time for a typical ELM from the configuration study described in Section 3. The overshoot in ΔW is due to vessel shielding effects.

It was shown in Section 3 that Type I ELMs are inherent to non-seeded discharges well above threshold, where good confinement and low Z_{eff} are obtained. It is thus important to understand the energy and particle loss per ELM, and the timescales associated with them, in order to assess their impact on divertor components. Figure 12 shows the total particle inventory and stored energy on a fast time scale for a typical isolated ELM. The stored energy drops extremely rapidly, on a time scale of 100-200 μsec, characteristic of parallel heat conduction. The particle inventory drop occurs more slowly, on the scale of a few milliseconds, characteristic of particle flow times in the SOL. It appears thus that the energy is conducted very quickly along the field lines to the target, with the particle efflux following the primary conduction-dominated energy dump. Figure 13 shows the percentage drop in density and energy, respectively, for 10 pulses from the database described in Section 3.2. Five of the pulses, representing five of the configurations studied, had no puffing, with a corresponding set for pulses with a moderate puff rate of 1 x 10^{22} s^{-1}, which is sufficiently low to have only a small effect on the ELM frequency. It can be seen that there is a general trend for the percentage energy and density drops to decrease with increasing frequency, although the time averaged energy and particle loss from ELMs, obtained by multiplying the frequency times the drops, increases with ELM frequency. Thus the low frequency, higher triangularity discharges lose less energy through ELMs in a time-averaged sense, but the individual ELMs are larger and thus potentially more damaging to the divertor plates. By increasing the puffing rate, the ELM frequency can be made larger, and the fractional energy loss per ELM can be reduced further, to about 2% in our discharges. This comes, however, at the expense of confinement, as illustrated in Fig.14. Even higher puffing causes a transition from Type I to grassy ELMs, with a further decrease in confinement to enhanced L-mode values.

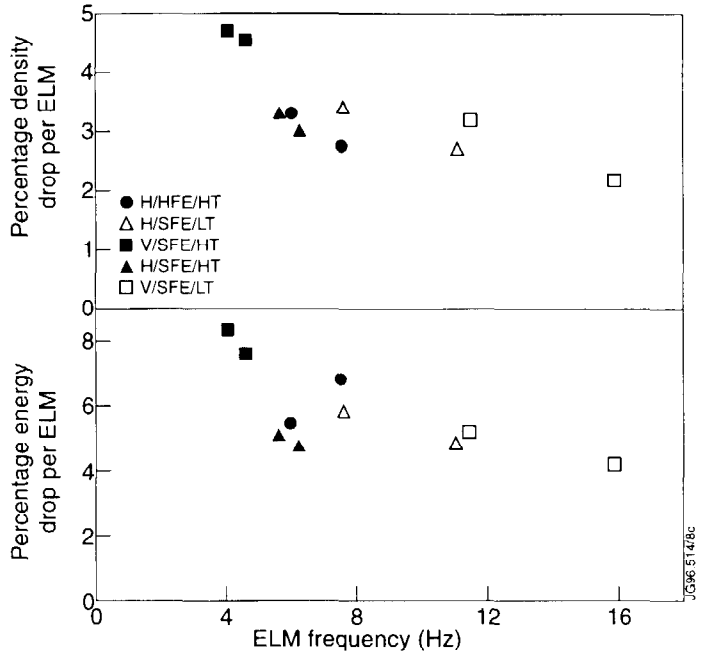

Fig.13 Percentage density drop (top) and energy drop (bottom) per ELM vs. ELM frequency for pulses from the configuration study of Section 3.

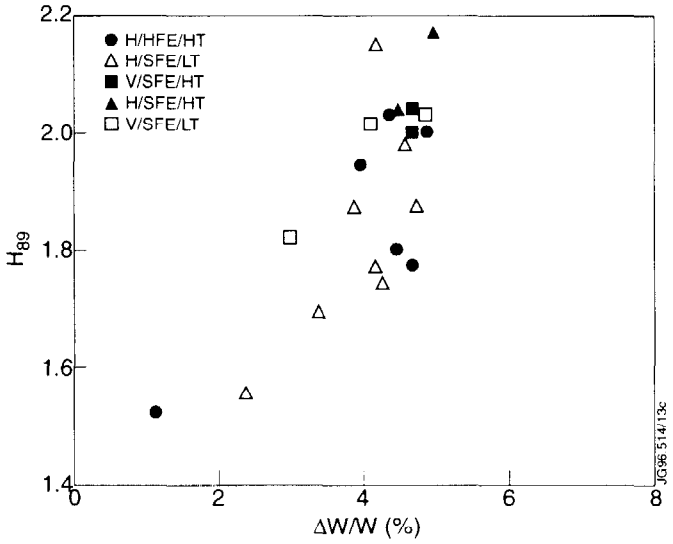

Fig.14 The confinement quality H_{89} vs. percentage energy drop per ELM, ΔW/W, for the beam fuelled and D_2 puffed pulses of the configuration study.

Energy deposition on the ITER target plates of greater than about 1% of the stored energy is expected to cause severe erosion [10]. Fast Langmuir probe studies in JET show a very fast, short lived deposition of particles displaced by up to 20 cm from the pre-ELM strike point position, followed by a high-recycling deposition of particles at the original strike zones which lasts a few milliseconds, as shown in Fig.15 for an ELM on the vertical plates. Full cross section CCD views indicate that the ELM also produces a great deal of D_α radiation at the main chamber limiters and upper dump plates. Because of the relatively slow time resolution of the JET infrared cameras and bolometers, however, it is not possible to determine precisely the fraction of the energy leaving the main plasma which

reaches the plates. It is known, however, that the ELM energy which does reach the plates is shifted and distributed over a larger area than that arriving between ELMs. More detailed quantification of the deposition of the ELM energy in JET must thus await more refined measurements and further analysis.

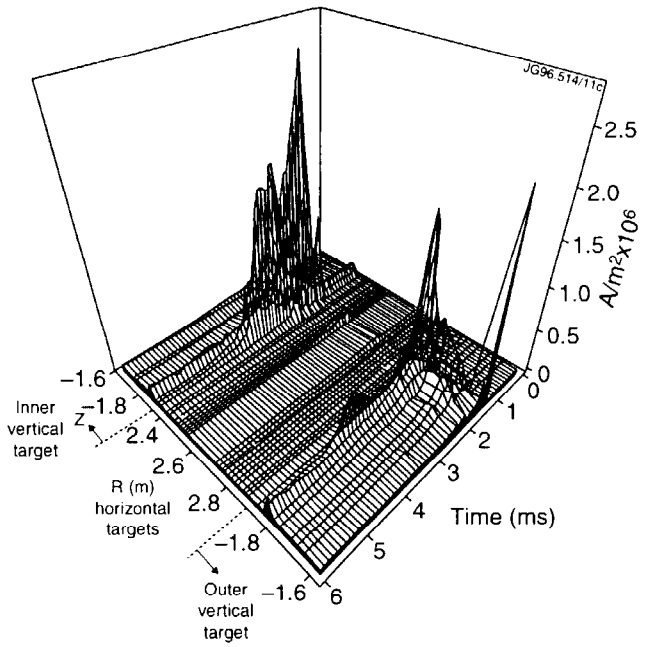

Fig.15 Unfolded 3-D plot of fast Langmuir probe ion saturation current measurement during an ELM on the vertical target.

5. CONCLUSIONS AND IMPLICATIONS FOR ITER

Compared with Mk I, the geometrically more closed Mark IIA configuration produces higher neutral pressures with correspondingly higher pumping rates, and facilitates access to the high recycling and detached plasma regimes. Although the density limit in Mk IIA is lower in ohmic and low power L-mode plasmas, it remains, as in Mk I, at roughly the Greenwald limit for H-mode pulses. The expected reduction in intrinsic impurity level in Mark IIA has not been observed, and this is believed to be due, at least in part, to bypass leakages.

For fixed power, field, and current, the ELM frequency in Type I ELMy H-mode discharges can be increased by a factor of several by decreasing the triangularity from 0.32 to 0.19, with no loss in confinement quality. The energy loss per ELM varies from about 8% to 4% as the triangularity is reduced. Further increase of the ELM frequency and decrease of amplitude, down to about 1%, was obtained by heavy D_2 puffing, but at the expense of confinement. However, ELMs somewhat larger than 1% may be acceptable to ITER, as the fraction of the ELM-expelled energy which reaches the plates is not yet well known in JET.

Differences which arise from target orientation (vertical vs. horizontal) at fixed flux expansion and triangularity appear to be quite small; both offer good confinement and plasma purity in the Type I ELMy H-mode operating regime. On the horizontal plate, large flux expansion resulted in slightly higher achievable main plasma densities, but poorer confinement and higher contamination by the intrinsic impurities. This may be due to the ELMs extending beyond the edge of the divertor.

Mark IIA operation with radiative power fractions greater than 0.5, achieved by seeding with N_2 or Neon, produced confinement degraded to a level

probably not acceptable for ITER, with high Z_{eff}, as had been found in Mk I. In this series of pulses, the vertical targets showed poorer confinement at a given f_{rad}, and were not capable of going to as high values of f_{rad}.

In summary, if the L→H power threshold in ITER is such that the Type I ELMy H-mode regime can be achieved, it appears to offer high confinement and low Z_{eff}, relative to the high radiated power fraction regime. The energy deposited on the plates between ELMs for the oberved radiated power fractions would be acceptable for ITER, but the deposition pattern of the ELM energy needs further study.

REFERENCES

[1] THE JET TEAM (presented by G.F. Matthews) Plasma Phys. Control. Fusion **37** (1995) A227.
[2] NEUHAUSER, J., et. al., ibid., A37.
[3] ITAMI, K., and THE JT-60 TEAM, ibid., A255.
[4] ALLEN, S.L., et. al., ibid., A191.
[5] VLASES, G.C., et. al., to be published in J. Nucl. Mater. (Proc. 12th Int. Conf. on Plasma Surface Interactions, San Raphael, 1996).
[6] LOARTE, A., and MONK, R., to be published
[7] THE JET TEAM (presented by D. Stork), IAEA-CN-64/A1-1, this Conference.
[8] THE JET TEAM (presented by L.D. Horton), paper presented at 23rd Eur. Conf. Kiev, 1996 (to be published in Plasma Phys. and Control. Fusion).
[9] MATTHEWS, G., et. al., to be published in J. Nucl. Mater. (Proc. 12th Int. Conf. on Plasma Surface Interactions, San Raphael, 1996).
[10] ITER-JCT AND HOME TEAMS (presented by G. Janeschitz) Plasma Phys. Control. Fusion **37** (1995) A19.